Diagrammatic analysis of multiphoton processes in a ladder-type three-level atomic system

Heung-Ryoul Noh[1,*] and Han Seb Moon[2,†]
[1]*Department of Physics, Chonnam National University, Gwangju 500-757, Korea*
[2]*Department of Physics, Pusan National University, Busan 609-735, Korea*
(Received 22 June 2011; published 14 November 2011)

We present a diagrammatic method for complete characterization of multiphoton processes in three-level atomic systems. By considering the interaction routes of the coupling and probe photons for a ladder-type, three-level, noncycling (or cycling) atomic system, we are able to completely discriminate between the pure one-photon and the pure two-photon resonance effects, and the effect of their combination in electromagnetically induced transparency (EIT) using our diagrammatic method. We show that the proposed diagrammatic method is very useful for the analysis of multiphoton processes in ladder-type EIT.

DOI: 10.1103/PhysRevA.84.053827 PACS number(s): 42.50.Gy, 32.80.Qk, 32.80.Wr

Quantum interference is a ubiquitous phenomenon in physics. In particular, electromagnetically induced transparency (EIT) in an atomic system is a quantum interference phenomenon of two pathways between two dipole-forbidden atomic states [1,2]. After the first proposal [3] and experimental realization [4], EIT has drawn considerable interest in the atomic and optical physics fields. This is because it can be applied to many valuable researches such as quantum information [5], light storage [6], and precision magnetometer [7]. EIT was investigated for many atomic species such as Rb, Na, or Cs [8–14] and for a variety of laser configuration [Λ, V, and ladder (or cascade) system] [1]. Of these configurations, ladder scheme has drawn much interest recently owing to its applications such as coherent control of polarization [15], study of Rydberg states [16], and multiwave mixing [17].

The effect of quantum interference in EIT has been investigated considerably from the first proposal report [3]. It should be noted that the underlying mechanism of EIT is closely related to Fano-interference phenomenon in atomic systems [18]. In reality, the effect of the probe beam is considered only in the first order the Rabi frequency of the probe beam, whereas that of the coupling beam is considered in all orders of the coupling beam Rabi frequency [9]. Furthermore, up to the second order in the Rabi frequency of the coupling beam, the line shape of EIT can be accurately understood by considering only two paths: one is direct way (one-photon coherence) and the other is indirect way via an intermediate state (three-photon coherence) [10]. However, when the probe beam intensity is comparable to the coupling beam intensity, the line shape in EIT shows a variety of variation and there occur many multiphoton processes. The line shape of EIT in this regime was studied in several papers [10,19,20]. Although the EIT spectrum in the strong probe regime was investigated previously, an accurate calculation and characterization of the multiphoton processes in three-level atomic system has not been reported.

Recently, theoretical studies on three-level ladder-type atoms [21,22] and experimental works for Na [13] and Rb [23,24] were reported. In particular we discriminated the EIT spectrum in terms of one-photon and two-photon coherence effects [22]. Although we could explain the spectrum successfully, the one-photon resonance effect comprises two-photon resonance effects simultaneously, and *vice versa*. In this paper we report an accurate discrimination of multiphoton processes existing in the EIT by employing an open ladder-type three-level atomic system. We could discriminate the EIT spectrum (background subtracted) into three parts: one is two-step excitation contribution (one-photon resonance term) [25], the next is two-photon resonance term, the last one is the mixed term of one-photon and two-photon resonances.

Figure 1(a) shows the energy level diagram for a ladder-type atomic system with noncycling transitions. The probe laser of wavelength λ_1 is tuned to the transition line between the ground ($|1\rangle$) and the intermediate ($|2\rangle$) states, whereas the coupling laser of wavelength λ_2 is tuned between the intermediate and the excited ($|3\rangle$) states. We also make assumptions about the branching ratios b_1 and b_2. In the calculation we assume that $\lambda_1 = 780$ nm and $\lambda_2 = 775.8$ nm, which are the resonance wavelengths for the transitions $5S_{1/2}$–$5P_{3/2}$ and $5P_{3/2}$–$5D_{5/2,3/2}$ of rubidium, respectively. Also the decay rates are $\gamma_1 = 2\pi \times 6$ MHz [26] and $\gamma_2 = 2\pi \times 0.97$ MHz [9].

The density-matrix equations are given by

$$\dot{\rho}_{33} = -\gamma_2\rho_{33} - \Omega_2 \mathrm{Im}\rho_{32}, \tag{1a}$$

$$\dot{\rho}_{22} = b_2\gamma_2\rho_{33} - \gamma_1\rho_{22} + \Omega_2 \mathrm{Im}\rho_{32} - \Omega_1 \mathrm{Im}\rho_{21}, \tag{1b}$$

$$\dot{\rho}_{11} = b_1\gamma_1\rho_{22} + \Omega_1 \mathrm{Im}\rho_{21}, \tag{1c}$$

$$\dot{\rho}_{32} = (i/2)[\Delta_2\rho_{32} + \Omega_1\rho_{31} + \Omega_2(\rho_{33} - \rho_{22})], \tag{1d}$$

$$\dot{\rho}_{31} = (i/2)[\Delta_0\rho_{31} + \Omega_1\rho_{32} - \Omega_2\rho_{21}], \tag{1e}$$

$$\dot{\rho}_{21} = (i/2)[\Delta_1\rho_{21} - \Omega_2\rho_{31} + \Omega_1(\rho_{22} - \rho_{11})], \tag{1f}$$

where $\rho_{ij} = \rho^*_{ji}$ $(i \neq j)$. $\Delta_1 = 2\delta_1 + i\gamma_1$, $\Delta_2 = 2\delta_2 + i(\gamma_1 + \gamma_2)$, and $\Delta_0 = 2(\delta_1 + \delta_2) + i\gamma_2$, where $\delta_{1(2)}$ and $\Omega_{1(2)}$ are the frequency detuning and the Rabi frequency of the probe (coupling) beam, respectively. The absorption coefficient of the probe beam, averaged over the Maxwell-Boltzmann velocity distribution and various transit times, is given by

$$\alpha = -N_{\mathrm{at}}\frac{3\lambda_1^2}{2\pi}\frac{\gamma_1}{\Omega_1}\frac{1}{t_{\mathrm{av}}}\int_0^{t_{\mathrm{av}}} dt \int_{-\infty}^{\infty} dv \frac{e^{-(v/u)^2}}{\sqrt{\pi}u}\mathrm{Im}\rho_{21}, \tag{2}$$

where $\delta_1 = \delta_p - (2\pi/\lambda_1)v$, $\delta_2 = \delta_c + (2\pi/\lambda_2)v$ [$\delta_{p(c)}$: the detuning of the probe (coupling) beam], u is the most probable

*hrnoh@chonnam.ac.kr
†hsmoon@pusan.ac.kr

 ©2011 American Physical Society

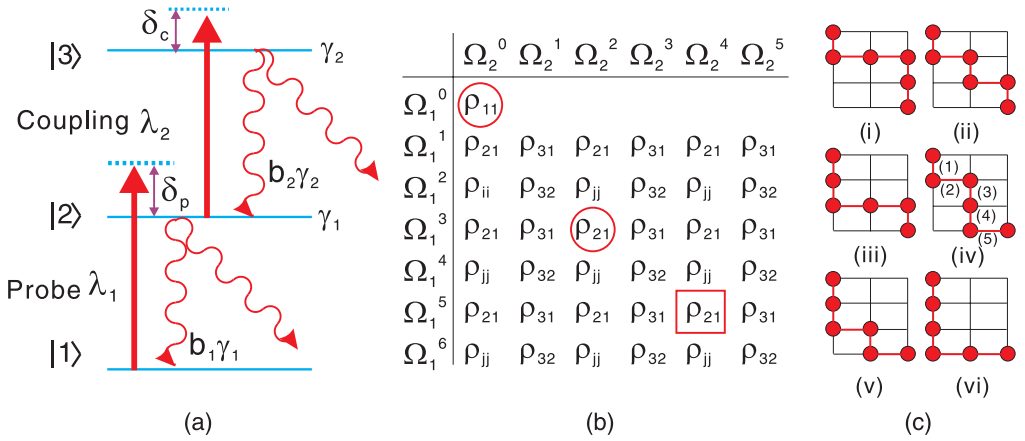

FIG. 1. (Color online) (a) Energy level diagram for three-level ladder systems. (b) Diagram for matrix elements for the coupling and probe Rabi frequencies. (c) Six possible routes for arriving at the element of $\Omega_1^3\Omega_2^2$.

speed of the atom, and $t_{\rm av}$ is the average transit time [22]. Since the transmittance is given approximately by $e^{-\alpha l}$ (l: the length of the cell), it is approximately proportional to the averaged $\mathrm{Im}\rho_{21}$. Therefore, in what follows we discuss the transmittance spectrum in terms of the averaged $\mathrm{Im}\rho_{21}$.

Using Eq. (1f), $\mathrm{Im}\rho_{21}$ can be decomposed into two parts:

$$\mathrm{Im}\rho_{21} = \mathrm{Im}\left[\frac{\Omega_1}{\Delta_1}(\rho_{11}-\rho_{22})\right] + \mathrm{Im}\left[\frac{\Omega_2}{\Delta_1}\rho_{31}\right]. \tag{3}$$

Since the former and the latter terms on the right-hand side in Eq. (3) are related to the population difference and two-photon coherence, respectively, these two are roughly regarded as one-photon and two-photon coherence terms, respectively [22]. However, although the latter term refers to the two-photon coherence ρ_{31}, it really possesses the contributions from both one-photon and two-photon resonances. It is a similar case for the population difference term. Here we separate the total signal into three terms: one is a purely one-photon resonance term, the second is a purely two-photon resonance term, the last one is a mixed term of one-photon and two-photon resonances.

In order to understand and accurately discriminate between the pure one-photon and two-photon resonance effects, we plot the density matrix elements for different orders of the Rabi frequencies of the probe and coupling lasers as shown in Fig. 1(b). Figure 1(b) was obtained by expanding the density-matrix elements in the orders of Ω_1 and Ω_2. In Fig. 1(b) i denotes the populations ρ_{11} and ρ_{22}, while j represents the populations ρ_{11}, ρ_{22}, and ρ_{33}. The meaning of Fig. 1(b) is very clear. For instance, ρ_{11} has the components in the orders of $\Omega_1^0\Omega_2^0$, $\Omega_1^2\Omega_2^0$, $\Omega_1^2\Omega_2^2$, etc. Note that the lowest order term of ρ_{11} is 1, which is independent of the branching ratios of the system.

Since we measure the transmittance of the probe laser beam, it is necessary to add all values of ρ_{21} in Fig. 1(b). Let us concentrate on the term of ρ_{21} in the order of $\Omega_1^3\Omega_2^2$. There are many routes to arrive at this point from the lowest order of ρ_{11}. In Fig. 1(c) we show six possible routes. The three routes (i), (ii), and (iii) take downward propagation in the last step, which corresponds to population difference term in Eq. (3). In contrast, three routes (iv), (v), and (vi) take the right direction in the last step, which correspond to the coherence term in Eq. (3). Among the three routes (i), (ii), and (iii), only route (iii) does not pass the point of ρ_{31}, which implies a two-photon resonance process. Therefore, only route (iii) represents the pure one-photon resonance effect, in other words, a two-step excitation in the process [13]. We can also see that only path (iv) does not pass the population term. Consequently, we see that the path (iv) implies a pure two-photon process. The other paths (i), (ii), (v), and (vi) represent the mixed effects of one-photon and two-photon resonances. As an example we can write ρ_{21} in the order of $\Omega_1^2\Omega_2^3$ via the path (iv) as follows:

$$\rho_{21}^{(\mathrm{iv})} = \left(\frac{\Omega_2}{\Delta_1}\right)\left(\frac{-\Omega_1}{\Delta_0}\right)\left(\frac{-\Omega_1}{\Delta_2}\right)\left(\frac{\Omega_2}{\Delta_0}\right)\left(\frac{\Omega_1}{\Delta_1}\right)1, \tag{4}$$

where 1 implies the population $\rho_{11}=1$ in the order of $\Omega_1^0\Omega_2^0$, and the five successive terms from the right represent the interactions (1), (2), (3), (4), and (5) in Fig. 1(c), respectively. We can write similar equations for other paths when the atomic system is cycling.

We first consider the one-photon resonance effect. It is easy to recognize that the pure one-photon resonance effect can be obtained by setting ρ_{31} zero. This process is merely to set up the rate equations, which are explicitly given by [22]

$$\dot\rho_{33}^{(0)} = -\gamma_2\rho_{33}^{(0)} - \frac{(\gamma_1+\gamma_2)\Omega_2^2}{4\delta_2^2+(\gamma_1+\gamma_2)^2}\left(\rho_{33}^{(0)}-\rho_{22}^{(0)}\right), \tag{5a}$$

$$\dot\rho_{22}^{(0)} = b_2\gamma_2\rho_{33}^{(0)} - \gamma_1\rho_{22}^{(0)} + \frac{(\gamma_1+\gamma_2)\Omega_2^2}{4\delta_2^2+(\gamma_1+\gamma_2)^2}\left(\rho_{33}^{(0)}-\rho_{22}^{(0)}\right) - \frac{\gamma_1\Omega_1^2}{4\delta_1^2+\gamma_1^2}\left(\rho_{22}^{(0)}-\rho_{11}^{(0)}\right), \tag{5b}$$

$$\dot\rho_{11}^{(0)} = b_1\gamma_1\rho_{22}^{(0)} + \frac{\gamma_1\Omega_1^2}{4\delta_1^2+\gamma_1^2}\left(\rho_{22}^{(0)}-\rho_{11}^{(0)}\right), \tag{5c}$$

where $\rho_{ii}^{(0)}$ $(i=1,2,3)$ represents the populations in the absence of the coherence ρ_{31}. Thus the pure one-photon resonance effect is given by

$$L_{1\mathrm{p}} = \mathrm{Im}\left[\frac{\Omega_1}{\Delta_1}\left(\rho_{11}^{(0)}-\rho_{22}^{(0)}\right)\right], \tag{6}$$

where L implies a "lower transition" for the probe beam. It should be noted that this one-photon resonance term belongs to the population term in Eq. (3) not to the coherence term.

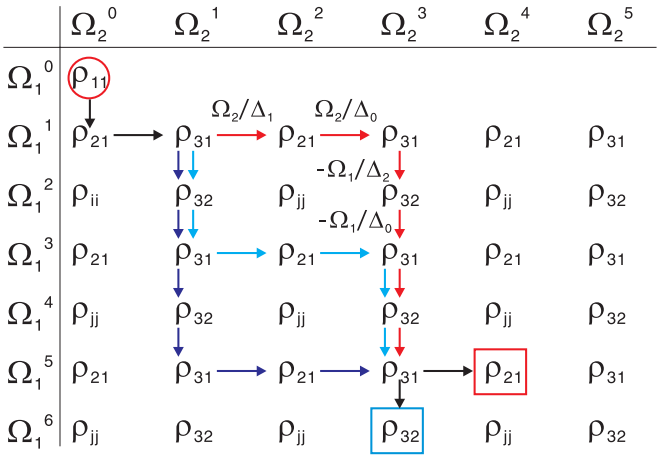

FIG. 2. (Color online) Three routes for pure two-photon resonance to the element of $\Omega_1^5\Omega_2^4$.

Therefore the other part, except for L_{1p}, in Eq. (3) represents the mixed term, which will be discussed later.

Now we consider the two-photon resonance term. The multiplication factor such as Ω_2/Δ_1, shown in Fig. 2, acts as, for example, $\rho_{31}(\Omega_2/\Delta_1) = \rho_{21}$, which can be derived easily from Eqs. (1d)–(1f). When both the coupling and probe beams are weak, the two-photon coherence term is ρ_{21} in the order of $\Omega_1\Omega_2^2$. In contrast, the two-photon coherence term in the weak probe intensity limit, that is, up to the first order in Ω_1, is the sum of all ρ_{21} in the second row in Fig. 2. This is often discussed in papers on ladder-type EIT [9]. However, when the intensities of the coupling and probe beams are arbitrary, it is necessary to sum over all ρ_{21} in Fig. 2 except for the values in the first column, which constitute the background signal.

The calculation can be easily performed using the method shown in deriving Eq. (4). In the case of term ρ_{21} in the order of $\Omega_1\Omega_2^2$, it can be immediately obtained as $(-\Omega_1/\Delta_2)(\Omega_2/\Delta_0)(\Omega_1/\Delta_1)1$, because there is only one route to this point. Let us consider the term in the order of $\Omega_1^5\Omega_2^4$ marked as a rectangle in Fig. 2. As shown in Fig. 2 we have three possible routes. Each route contributes equally to the coherence term. Therefore we need to multiply by a factor of 3 in the calculated result. We can easily see that the number of possible routes to the term in the order of $\Omega_1^m\Omega_2^n$ is ${}_{(m+n-3)/2}C_{(m-1)/2}$. Therefore, using the variables $m = 2\mu + 1$ and $n = 2\nu + 2$ $(\mu, \nu = 0, 1, 2, \ldots)$, the result is given by

$$\frac{\Omega_2}{\Delta_1}\left[\sum_{\nu=0}^{\infty}\sum_{\mu=0}^{\infty}{}_{\mu+\nu}C_{\mu}x^{\mu}y^{\nu}\right]\left(\frac{\Omega_2}{\Delta_0}\right)\left(\frac{\Omega_1}{\Delta_1}\right)1, \tag{7}$$

where $x = \Omega_1^2/(\Delta_0\Delta_2)$ and $y = \Omega_2^2/(\Delta_0\Delta_1)$. Since $\sum_{\mu=0}^{\infty}\sum_{\nu=0}^{\infty}{}_{\mu+\nu}C_{\mu}\,x^{\mu}\,y^{\nu} = \sum_{\zeta=0}^{\infty}\sum_{\mu=0}^{\zeta}{}_{\zeta}C_{\mu}\,x^{\mu}\,y^{\zeta-\mu} = \sum_{\zeta=0}^{\infty}y^{\zeta}[1+(x/y)]^{\zeta} = 1/(1-x-y)$ in Eq. (7), the final result is given by

$$L_{2p} = \mathrm{Im}\left[\frac{\Delta_2\Omega_1\Omega_2^2}{\Delta_1\left(\Delta_0\Delta_1\Delta_2 - \Delta_1\Omega_1^2 - \Delta_2\Omega_2^2\right)}\right]. \tag{8}$$

The result in Eq. (8) can be also obtained by expressing the coherence term in Eq. (3) in terms of the populations as follows:

$$\mathrm{Im}\left[\frac{\Delta_1(\rho_{33}-\rho_{22}) - \Delta_2(\rho_{22}-\rho_{11})}{\Delta_1\left(\Delta_0\Delta_1\Delta_2 - \Delta_1\Omega_1^2 - \Delta_2\Omega_2^2\right)}\Omega_1\Omega_2^2\right]. \tag{9}$$

where Eqs. (1d)–(1f) have been used to calculate the coherence. Setting $\rho_{11} = 1$ and $\rho_{22} = \rho_{33} = 0$ in Eq. (9), we can obtain the same results as in Eq. (8). Therefore we can interpret the terms in the various orders of Ω_1 and Ω_2 by means of the corresponding many interaction pathways from the point $\Omega_1^0\Omega_2^0$ to the considered point.

The other contributions in $\mathrm{Im}\rho_{21}$ except for the one-photon resonance term in Eq. (6) and two-photon resonance term in Eq. (8) constitute the mixed term L_{mix}. Since the mixed term is very dependent on the populations, this can explain the dip and peak signals for various branching ratios, as discussed in Ref. [22].

Here we present a brief description of the results for the case where the upper transition is used as a probe line. In this case the measured signal is proportional to the following equation:

$$\mathrm{Im}\rho_{32} = \mathrm{Im}\left[\frac{\Omega_2}{\Delta_2}(\rho_{22}-\rho_{33})\right] + \mathrm{Im}\left[\frac{-\Omega_1}{\Delta_2}\rho_{31}\right]. \tag{10}$$

Also the one-photon and two-photon contributions are given by

$$U_{1p} = \mathrm{Im}\left[\frac{\Omega_2}{\Delta_2}\left(\rho_{22}^{(0)} - \rho_{33}^{(0)}\right)\right], \tag{11}$$

$$U_{2p} = \mathrm{Im}\left[\frac{-\Omega_1^2\Omega_2}{\Delta_0\Delta_1\Delta_2 - \Delta_1\Omega_1^2 - \Delta_2\Omega_2^2}\right], \tag{12}$$

respectively, where U implies the "upper transition" for the probe beam, and Eq. (12) was obtained by replacing Ω_2/Δ_1 in Eq. (7) with $-\Omega_1/\Delta_2$.

Figure 3(a) [3(b)] shows typical calculated results when $b_1 = 1$ and $b_2 = 0.75$ [$b_1 = 0.5$ and $b_2 = 0.5$]. In Fig. 3, $\delta_c = 0$, whereas δ_p is scanned. The Rabi frequencies are $\Omega_1 = 0.2\gamma_1$ and $\Omega_2 = 5.0\gamma_2$. In Fig. 3, (i) shows the total, one-photon resonance, and the background signals. (ii) shows a detailed plot near the frequency origin. (iii) shows the two-photon resonance term and the mixed term. The background signal was obtained at the condition of $\Omega_2 = 0$. The one-photon resonance signal is very broad and weak compared to the other signals. In Fig. 3 we can see that the broad peak or dip signal results mostly from the mixed term. In contrast, a narrow transmittance signal results from the two-photon resonance term. Since the mixed term contains the effect of the populations, it can be broadened due to the ac Stark shift and depends heavily on the branching ratios. Thus the optical pumping affects the signals via the mixed term. Because the two-photon resonance term does not contain the populations, it does not depend on the branching ratios.

In this article we present a simple diagrammatic method for the accurate characterization of multiphoton processes which occur in EIT for three-level ladder systems at arbitrary intensities of the probe and the coupling beam and with arbitrary branching ratios. The line shape can be decomposed into three components: the pure one-photon resonance, the pure two-photon resonance, and the mixed contribution of both. We explained each process by means of a diagrammatic method, which facilitates the clear understanding of the interaction

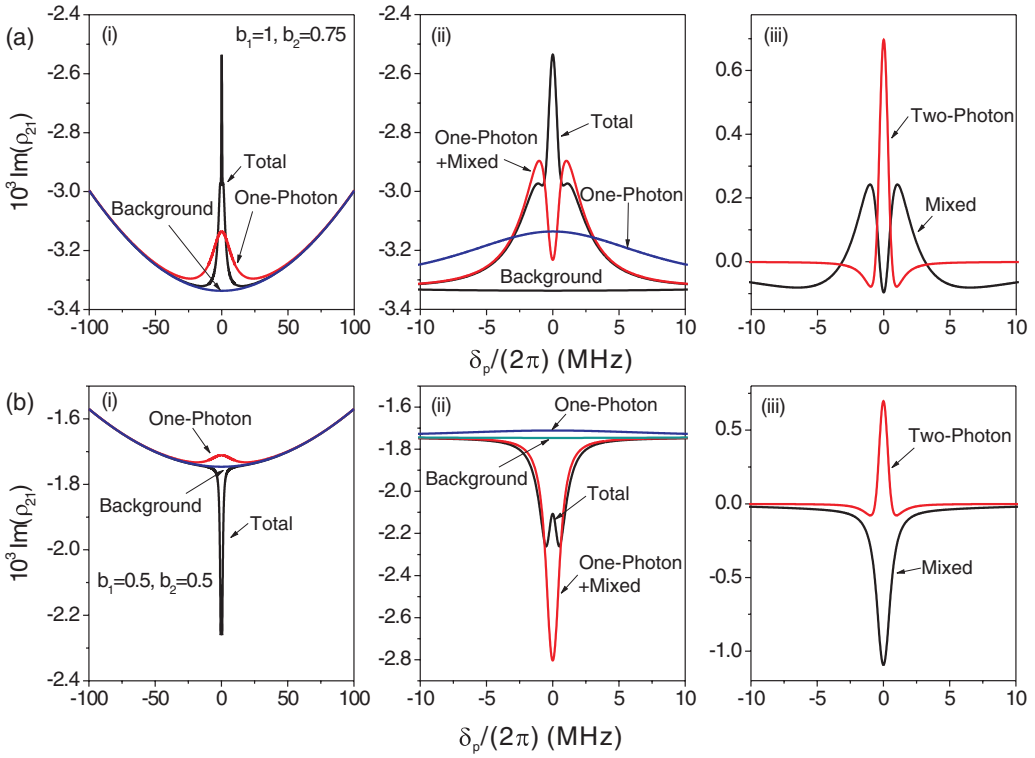

FIG. 3. (Color online) Typical calculated EIT spectra when (a) $b_1 = 1$ and $b_2 = 0.75$ and (b) $b_1 = 0.5$ and $b_2 = 0.5$.

between atoms and lights. We found that the two-photon resonance signal maintains line shape regardless of the branching ratios, whereas the mixed term, which is strongly dependent on the branching ratios, determines overall line shape in the spectrum. The diagrammatic method described in this letter can be generally applied to calculation of line shapes in other geometries such as Λ-, V-type, N-type, or even real atoms.

This research was supported by Basic Science Research Program through the National Research Foundation of Korea (NRF) funded by the Ministry of Education, Science and Technology (No. 2011-0009886). Also, this work was supported by the Korea Science and Engineering Foundation (KOSEF) grant funded by the Korea government (MOST) (No. R01-2007-000-11636-0).

[1] M. Fleischhauer, A. Imamoglu, and J. P. Marangos, Rev. Mod. Phys. **77**, 633 (2005).
[2] J. P. Marangos, J. Mod. Opt. **45**, 471 (1998).
[3] S. E. Harris, J. E. Field, and A. Imamoglu, Phys. Rev. Lett. **64**, 1107 (1990).
[4] K. J. Boller, A. Imamoglu, and S. E. Harris, Phys. Rev. Lett. **66**, 2593 (1991).
[5] K. Hammerer, A. S. Sørensen, and E. S. Polzik, Rev. Mod. Phys. **82**, 1041 (2010).
[6] M. D. Lukin, Rev. Mod. Phys. **75**, 457 (2003).
[7] D. Budker and M. V. Romalis, Nat. Phys. **3**, 227 (2007).
[8] R. R. Moseley, S. Shepherd, D. J. Fulton, B. D. Sinclair, and M. H. Dunn, Opt. Commun. **119**, 61 (1995).
[9] J. Gea-Banacloche, Y. Q. Li, S. Z. Jin, and M. Xiao, Phys. Rev. A **51**, 576 (1995).
[10] S. Wielandy and A. L. Gaeta, Phys. Rev. A **58**, 2500 (1998).
[11] D. McGloin, M. H. Dunn, and D. J. Fulton, Phys. Rev. A **62**, 053802 (2000).
[12] S. D. Badger, I. G. Hughes, and C. S. Adams, J. Phys. B **34**, L749 (2001).
[13] N. Hayashi, A. Fujisawa, H. Kido, K. Takahashi, and M. Mitsunaga, J. Opt. Soc. Am. B **27**, 1645 (2010).
[14] J. J. Clarke, W. A. van Wijngaarden, and H. Chen, Phys. Rev. A **64**, 023818 (2001).
[15] R. Drampyan, S. Pustelny, and W. Gawlik, Phys. Rev. A **80**, 033815 (2009).
[16] M. Saffman, T. G. Walker, and K. Mølmer, Rev. Mod. Phys. **82**, 2313 (2010).
[17] Y. Zhang, U. Khadka, B. Anderson, and M. Xiao, Phys. Rev. Lett. **102**, 013601 (2009).
[18] U. Fano, Phys. Rev. **124**, 1866 (1961).
[19] K. Pandey and V. Natarajan, J. Phys. B **41**, 185504 (2008).
[20] K. Pandey, D. Kaundilya, and V. Natarajan, Opt. Commun. **284**, 252 (2011).
[21] T. Y. Abi-Salloum, J. Mod. Opt. **57**, 1366 (2010).
[22] H. R. Noh and H. S. Moon, Opt. Express **19**, 11128 (2011).
[23] H. S. Moon, L. Lee, and J. B. Kim, Opt. Express **16**, 12163 (2008).
[24] H. S. Moon and H. R. Noh, J. Phys. B **44**, 055004 (2011).
[25] P. R. Berman and V. S. Malinovsky, *Principles of Laser Spectroscopy and Quantum Optics* (Princeton University Press, Princeton, 2011).
[26] P. Siddons, C. S. Adams, C. Ge, and I. G. Hughes, J. Phys. B **41**, 155004 (2008).